High Noon for Mobile Networks: Short-Time EMF Measurements to Capture Daily Exposure

Sara Adda, Luca Chiaraviglio, *Senior Member, IEEE*, Daniele Franci, Chiara Lodovisi, Nicola Pasquino, *Senior Member, IEEE*, Settimio Pavoncello, Chiara Pedroli, and Renata Pelosini

***Abstract*—Exposure from radio base stations (BSs) is often only monitored over short periods, typically during the daily hours of working days. However, BS exposure can vary throughout the day and even between working days and weekends or holidays. The objective of this study is to determine to what extent short-term exposure measurements taken during daily hours are representative of daily average exposure levels. To achieve this goal, we analyzed a set of long-term measurements taken by monitoring units located in sensitive areas, which are characterized by a homogeneous distribution of users over working hours, such as hospitals, train stations, and university centers. Our results reveal that 6-min measurements taken on working days can overestimate the average exposure level over 24 h if taken over a wider time interval than that commonly considered for peak traffic and, therefore, higher exposure. Based on the common pattern of exposure over time in various locations, an extrapolation factor is proposed to predict daily exposure levels from short-time measurements.**

***Index Terms*—4G long term evolution (LTE), 5G new radio (NR), electromagnetic field (EMF) monitoring, extrapolation factor, human exposure, measurements, wideband monitoring.**

I. Introduction

HUMAN exposure to radio frequency (RF) electromagnetic field (EMF) is the topic of specific guidelines that suggest frequency-based limits for both general public and occupational exposure. In 2020, the International Commission on Non-Ionizing Radiation Protection (ICNIRP) has released a revision [1] of its guidelines first published in 1998 [2], focusing on the RF range between 100 kHz and 300 GHz.

Manuscript received 21 June 2023; revised 14 September 2023; accepted 29 September 2023. Date of publication 13 October 2023; date of current version 26 October 2023. This work was supported by the PLAN-EMF Project [King Abdullah University of Science and Technology (KAUST)-National Inter-University Consortium for Telecommunications (CNIT)] under Award OSR-2020-CRG9-4377. The Associate Editor coordinating the review process was Dr. Sergio Rapuano. *(Corresponding author: Nicola Pasquino.)*

Sara Adda, Chiara Pedroli, and Renata Pelosini are with the Dipartimento Rischi Fisici e Tecnologici, Regional Agency for Environmental Protection of Piedmont (ARPA Piemonte), Ivrea, 10015 Turin, Italy (e-mail: sara.adda@arpa.piemonte.it; chiara.pedroli@arpa.piemonte.it; renata.pelosini@arpa.piemonte.it).

Luca Chiaraviglio and Chiara Lodovisi are with the National Inter-University Consortium for Telecommunications (CNIT), 43124 Parma, Italy, and also with the Department of Electronic Engineering, University of Rome "Tor Vergata," 00133 Rome, Italy (e-mail: luca.chiaraviglio@uniroma2.it; chiara.lodovisi@uniroma2.it).

Daniele Franci and Settimio Pavoncello are with ARPA Lazio, 00173 Rome, Italy (e-mail: daniele.franci@arpalazio.it; settimio.pavoncello@arpalazio.it).

Nicola Pasquino is with the Dipartimento di Ingegneria Elettrica e delle Tecnologie dell'Informazione, Università degli Studi di Napoli Federico II, 80125 Naples, Italy (e-mail: nicola.pasquino@unina.it).

Digital Object Identifier 10.1109/TIM.2023.3324354

Various monitoring activities are carried out worldwide to assess compliance of exposure with limits set by national and international guidelines and regulations [3], [4], [5], [6]. The Serbian EMF RATEL system [7], [8], for example, is a nationwide long-term monitoring system including about 100 probes covering most cities, although short-term monitoring campaigns are more widely adopted because they allow covering a wider area with the same number of probes.

One relevant aspect of exposure monitoring is the averaging time. While RF monitoring usually relies on the root mean square (rms) value of the electric field as the main quantity for large-scale environmental monitoring, different averaging times are used to assess the field strength. European guidelines [2] and the Recommendation by the European Council issued in 1999 [9] suggest 6-min averaging, while the updated version issued in 2020 [1] suggest that 30 min are used. National laws may introduce additional reference intervals. As an example, Italy requires that *exposure limits* are averaged over 6 min [10], while *attention values* and *quality objectives* are evaluated over 24 h [11].

The issue of time variability and averaging time is of particular importance in the case of exposure to EMFs emitted by base stations (BSs), due to the variability of emitted power related to network loads management [12], [13], [14], [15] and, for 5G new radio (NR) systems, also to the temporal beam management functionalities [16], [17]. Furthermore, 5G pilot signals can show temporal variations, mainly due to changes introduced in the propagation conditions [18].

Because of variability, short-time measurements of exposure levels near BS sites could be not representative of long-term exposure, which is an important parameter in epidemiological studies [19]. In addition, the comparison of EMF levels to exposure limits in the case of averaging over time intervals longer than 6 min is a mandatory step for different exposure regulations [19]. Surprisingly, a few studies have investigated the relationship between short- and long-term measurements and exposure parameters, performing some analysis on signals radiated by pre-5G systems [20], [21] and/or in a limited number of exposure contexts [22].

The goal of this work is to introduce a method to investigate the relationship between short-time measurements and daily exposure levels, over measurement sites subject to variegate exposure conditions. Based on the results of the analysis, we introduce an extrapolation factor to predict daily exposure levels from short-time measurements for urban environments characterized by a homogeneous distribution of users over the daily hours.

The article is organized as follows. Section II sheds light on the positioning of our work, by analyzing the relevant literature. In Section III, the measurement system and methodology are presented. Section IV details the experimental results. Section V formally defines the extrapolation factor to correlate 6 and 30 min (i.e., short-term) measurements with 24-h (i.e., long-term) averages. Section VI briefly discusses the applications of our work. Finally, conclusions and future work are drawn in Section VII.

II. Related Work

The analysis of the temporal exposure variations is a central aspect of EMF monitoring in mobile networks. Several EMF monitoring initiatives are currently ongoing across Europe [3], [7], [8], mainly lead by the agencies in charge of controlling the EMF levels over the territory. The observation of such trends over different time scales (hour, day, and week) allows for ensuring that the measured exposure levels are always within the maximum EMF limits imposed by law. Our work is instrumental for the activities performed by environmental protection agencies because we aim at reducing the amount of time needed to perform a continuous measurement in a single location while increasing the set of locations that can be monitored over a given temporal window.

At a research level, the temporal variation of exposure is tackled by works deploying exposimeters over the territory to retrieve EMF measurements [23], [24], [25], [26], [27]. More concretely, Frei et al. [23] collected exposure information with exposimeters kept by volunteers for one week. The collected data are then instrumental to compute average exposure values over specific intervals of time (weekly, daily, nighttime, and daytime). Birks et al. [24] targeted the EMF assessment over children, by extracting median exposure values from different microenvironments and different periods over the whole temporal measurement windows. Aerts et al. [25] analyzed over one year of measurements collected from an exposimeter-based network, by computing maximum and 90% variability of the exposure levels. More in depth, the proposed variability metric is extracted from the EMF temporal variation and the daily average. Velghe et al. [26] evaluated personal measurements with exposimeters from different microenvironments and different cities, by comparing exposure computed over rush hours against the other periods of time. In addition, a comparison between night hours and working hours is performed. Aerts et al. [27] reported the outcomes from a low-cost sensor network deployed over one year and a half. The considered metrics include the temporal variability, as well as more refined indicators like maximum exposure and the difference between maximum and minimum exposure over periods of time. In addition, daily and weekly EMF patterns are extracted, by considering also the effect of temporal smoothing.

Compared to [23], [24], [25], [26], and [27], our work is different in terms of methodology and scope. First, we employ monitoring units (not exposimeters), which are used by the environmental agencies appearing in this work to ensure legal compliance against the limits. A monitoring unit is a more complex device compared to an exposimeter and allows for obtaining more detailed and reliable exposure data. In addition, the adoption of monitoring units has an impact on the exposure assessment, for two main reasons: 1) each environmental protection agency owns a limited set of monitoring units and 2) each monitoring unit has to be controlled by an operator during the measurements, to protect the equipment from damage.

Moreover, a further point of discontinuity of our work compared to [23], [24], [25], [26], and [27] is the scope of temporal monitoring. In this work, we aim to develop and test an innovative methodology to estimate the average exposure over a given time period, by collecting exposure data over shorter time scales than the period selected for the average.

The second taxonomy of research includes the monitoring of control signals for network troubleshooting. For example, the work of Raida et al. [28] covers comprehensively the measurements of control signals [like the reference signal received power (RSRP)] over a long period of time. Obviously, the variation of RSRP is mainly due to a change in the propagation conditions, an aspect deeply covered also by the work of Chiaraviglio et al. [29]. Therefore, stability in the RSRP values is observed when the propagation conditions are kept unchanged [28]. Although we recognize the importance of monitoring control channels, our work is different in terms of scope because we focus on the exposure assessment of the whole spectrum used by mobile operators. In particular, the adopted monitoring units can measure the total exposure over a given location, which includes both the contributions of control channels (likely not varying over time) plus the traffic channels, which instead naturally exhibit strong variations between the different hours and the different days.

TABLE I
Measurement Sites and Number of Days Sampled

Country	ID	City	Location	no. days
IT	1	Rome	Dept. of Electronic Engineering	61
	2		University Hospital	61
	3	Turin	Polytechnic of Turin	60
	4		Train Station	23

III. Measurement System and Setup

Measurement sites were chosen in the urban areas of Rome and Turin, Italy (see Table I), characterized by the presence of BSs with different mobile technologies. The chosen sites also represent various spatial and temporal distributions of mobile users: the monitoring stations were installed in a University Department and a hospital in Rome and two areas close to a University and a railway station in Turin. All locations are, however, characterized by a similar exposure time trend over daily hours.

Measurement setups are shown in Fig. 1. In more detail, locations 1 and 2 are placed inside a building, close to the thin glass of the window, in line-of-sight, and at a distance of around 570 m from the closest radiating site. On the other

(a) (b) (c) (d)

Fig. 1. Measurement setups. (a) Location 1: Department of Electronic Engineering (Rome). (b) Location 2: University Hospital (Rome). (c) Location 3: Polytechnic of Turin (Turin). (d) Location 4: Train station (Turin).

hand, locations 3 and 4 are in the Turin urban area in the open air: the first one is in the city center on a terrace on the seventh floor in the same building where the BS is installed and the second one is on a balcony at the sixth floor at a distance of about 22 m from the nearest BS.

Time series no. 1, 2, and 4 were acquired during 2022, while time series no. 3 includes the beginning of the first pandemic lockdown in Italy (March 2020). The total length of each monitoring is shown in Table I.

Measurements were taken with two types of instruments.

1) In locations 1 and 2 (Rome), narrow-band monitoring stations were used. An Anritsu MS27102A Remote Spectrum Monitor working in the frequency range from 9 kHz to 6 GHz was connected through a type-N low-loss cable to a Keysight N6850A passive broadband omnidirectional antenna, with an operational band from 20 MHz to 6 GHz.
2) In locations 3 and 4 (Turin), a Narda 8059 wideband monitoring station with an electric field sensor working in the frequency band from 100 kHz to 7 GHz was used.

The wideband stations employed in locations 3 and 4 measure the total rms electric field level every 3 s and return as output the average value every 6 min. Data are saved on a remote FTP server once a day, by activating a modem for a short time interval (less than 1 min). Validation of the collected time series is then performed: data corresponding to 6-min intervals during which the modem is transmitting is removed and replaced by an interpolated value, to avoid the uplink contribution introduced by the modem transmission. Each 6-min trace is then postprocessed to compute the exposure average over 30-min intervals. In this way, we investigate the behavior of exposure according to the averaging time introduced by ICNIRP 2020 guidelines [1].

The narrow-band monitoring units employed in locations 1 and 2 work in a different way than the wideband stations of locations 3 and 4. More in depth, each monitoring unit is controlled by custom software running on an external unit, which is connected to the monitoring unit through an Ethernet connection, updating the measurement data on the cloud storage through an Internet connection. We refer the interested reader to [30] for the details of the measurement procedure, while here we provide a concise summary. In brief, the program synthesizes the measurement procedure as a sequence of Standard Commands for Programmable Instruments (SCPI), with the goal of sequentially monitoring a set of spectrum portions that is provided as input. The following operations are performed for each monitored band: 1) setting of spectrum analyzer commands; 2) sensing of the signal intensity to tune the reference level; 3) channel power (CP) recording; and 4) time-stamp association to each CP measurement and data logging. In this work, the monitored bands include all the spectrum portions in use by the main telecom operators in Italy (TIM, Vodafone, W3, Iliad, Opnet, and Fastweb) up to the N78 band.

A natural question here is: How much data was collected by the monitoring units? Actually, in our scenarios, the overall size of measured data is thin, that is, less than 2 MB per month, mainly because the whole iteration over the set of bandwidths requires 4–5 min to complete, yielding around 1–2 samples per band over each 6-min interval. Consequently, the size of each trace does not exceed 5 MB. The small size of the data should not be considered as a potential cause for the reduced significance of the analysis. In fact, samples span over a number of days (see Table I) that is large enough for the results to be statistically significant.

As a postprocessing step, we need to extract the total 6-min exposure from the CP-plus-timestamp measurement log of locations 1 and 2. To meet such a goal, we perform the following steps: 1) conversion from dBm to Watt of each CP sample; 2) data cleaning (i.e., removal of NaN or out-of-scale values); 3) data resampling with sampling rate set to 6 min for each band (with data aggregation type set as mean value); 4) data filling in case a 6-min interval does not have a value, in which case the filled data is expressed as the linear average between the two consecutive available data in the considered band; 5) data conversion from W to V/m to obtain the EMF exposure in each band and each 6-min interval (by applying the antenna effective area for the considered frequency band); and 6) root sum square of the EMF exposure samples from all monitored bands in a given 6-min interval in each band given an interval, to obtain the total exposure in V/m. Finally, similar to the postprocessing step applied to the wideband monitoring, an average over 30-min intervals is computed, again following the ICNIRP 2020 guidelines [1].

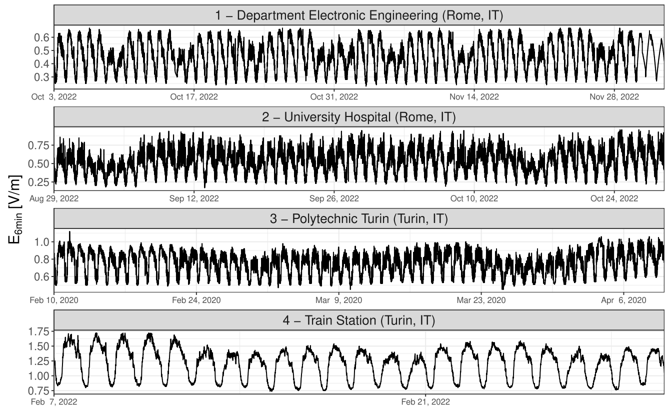

(a)

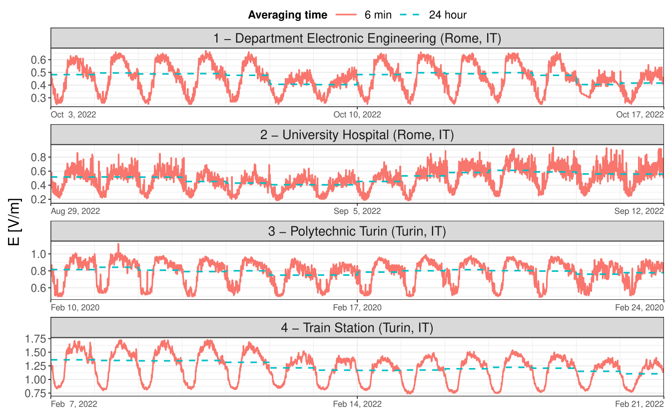

(b)

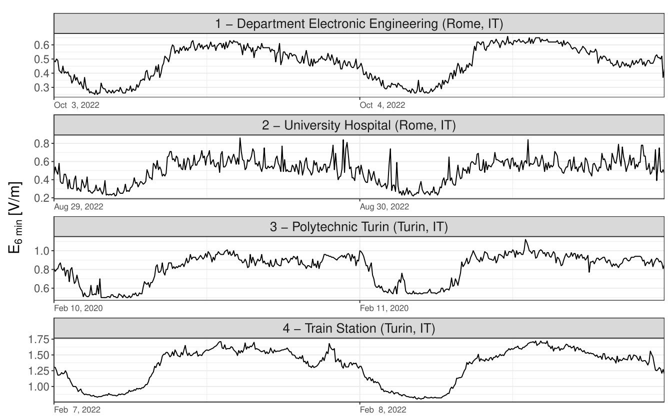

(c)

Fig. 2. Exposure patterns. (a) Whole-period monitoring. (b) Weekly pattern. (c) Daily pattern.

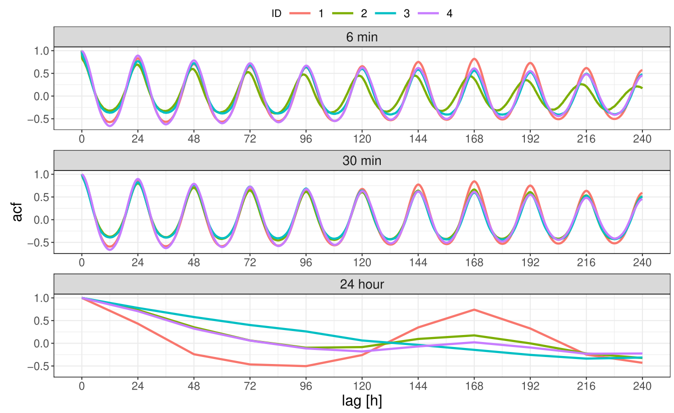

Fig. 3. Autocorrelation plots of time series.

IV. Experimental Results

A. Time Series

Fig. 2(a) shows the time series of the 6-min samples throughout the monitoring period at the four locations listed in Table I. A weekly [see Fig. 2(b)] pattern shows in all time series [31], where weekdays usually reach higher peaks than weekends, although the difference is more relevant in some locations than in others: see, for example, the apparent variations at location 1 (Rome, Department of Electronic Engineering) as opposed to location 3 (Turin, Polytechnic of Turin). Fig. 2(b) also shows the daily rms average (blue dashed line). The daily pattern in Fig. 2(c) confirms the expected behavior with high values during the day and low values at night, following the BS load. The figure also reveals that some locations have more significant short-term variations than others, like, for example, the University Hospital in Rome (location 2) compared to the Train Station in Turin (location 4).

B. Autocorrelation

Time patterns have been explored through the autocorrelation [32] plots shown in Fig. 3. Concerning 6- and 30-min averaging, all locations have peaks at multiples of 24 h, which confirms the presence of a daily pattern. Peaks keep higher than 0.5 for over ten days, which reveals a strong daily pattern. Negative peaks at –0.5 at multiples of 12 h show that the signal and its 12-h-delayed version are almost opposite in phase—a behavior that can be grasped also by observing Fig. 2(c).

Two peculiar situations occur. Autocorrelation of location 1 after one week reaches a higher peak ($\rho = 0.75$) than other locations ($\rho = 0.5$), which means that the similarity between two weeks is higher than that of other locations. This clearly shows in the 24-h-averaging autocorrelation plot, where ρ of location 1 at lag equal to 168 h (i.e., seven days) is the highest of all ($\rho = 0.75$). As a second key point, we can note that the periodicity of autocorrelation of location 2 is slightly less than 1 day. This is possibly due to a flaw in the clock of the measurement instrument used at that location, which caused a measured interval of 1 h to represent a slightly longer interval.

C. Sample Distribution

Boxplots [33] of samples averaged over 6 min, 30 min, and 24 h are shown in Fig. 4. Minor differences characterize the mean value of the three averaging times, while the variability of the 24-h samples is smaller than that of the other averaging intervals, as expected. A larger variance characterizes location 4 (i.e., Train Station in Turin, Italy).

In the considered locations, the maximum exposure limit is set to 6 V/m, which has to be compared against the average exposure over 24 h. This information can be retrieved from the blue boxplots of Fig. 4, which report the 24-h sample distributions. The maximum 24-h exposure is always lower than

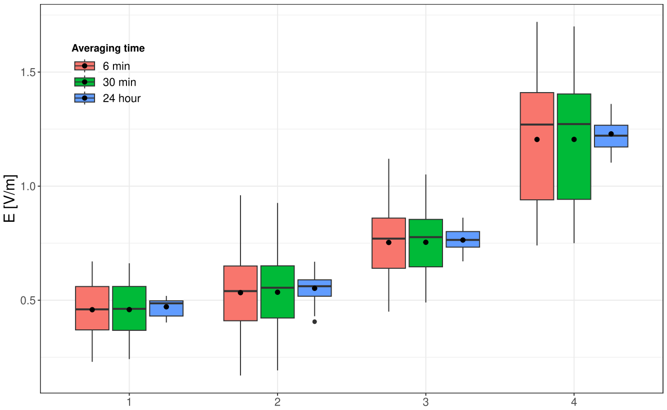

Fig. 4. 6-min, 30-min, and 24-h sample distribution throughout the monitoring period.

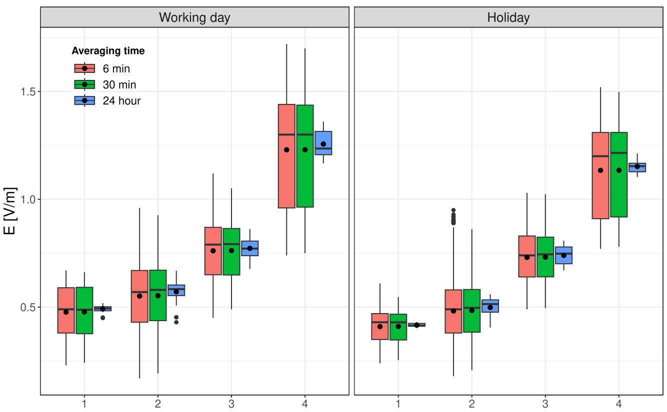

Fig. 5. 6-min, 30-min, and 24-h sample distribution for working days and holidays.

1.3 V/m, corresponding to 21% of the maximum permissible exposure.

To investigate further the weekly pattern observed in Fig. 2(b), Fig. 5 presents a comparison of the distributions of exposure samples for working days and holidays, where the latter includes both weekends and national holidays, given the similar behavior of the population during those days. The figure confirms that there is a decrease in the values of the distribution during holidays, at all locations.

To study the statistical significance of the observed differences we run an analysis of variance (ANOVA) test, whose results are shown in Table II. The reader is referred to [33] for a detailed explanation of all terms used in the table and all other statistical quantities appearing in the article. The test indicates that variations at different locations (*ID* term) are indeed significant ($p < 10^{-6}$) for all averaging times, confirming the intuition from the figure. ANOVA also highlights that whether a day is a holiday or a working day (*Holiday* term) changes the mean exposure significantly ($p < 10^{-6}$) and that there is a strong interaction ($p < 10^{-6}$) between *ID* and *Holiday*, which means that the entity of variations due to the different type of day depends on the specific location. The significance of the interaction is slightly smaller for the 24-h averaging time ($p = 10^{-2}$).

D. Relative Variation Over 24 h

The Italian law about the exposure of the general public to RF EMFs [10] sets the exposure limit at 6 V/m at all

TABLE II
ANOVA of Exposure for 6-min, 30-min, and 24-h Averaging Time

	Term	DoF	SS	MSS	F-stat	p-value
6 minutes	ID	3	2586.05	862.02	36953.80	$< 10^{-6}$
	Holiday	1	34.92	34.92	1497.03	$< 10^{-6}$
	ID:Holiday	3	4.15	1.38	59.30	$< 10^{-6}$
	Residuals	49017	1143.41	0.02		
30 minutes	ID	3	516.70	172.23	7917.77	$< 10^{-6}$
	Holiday	1	6.96	6.96	320.08	$< 10^{-6}$
	ID:Holiday	3	0.83	0.28	12.71	$< 10^{-6}$
	Residuals	9832	213.87	0.02		
24 hours	ID	3	10.97	3.66	2047.96	$< 10^{-6}$
	Holiday	1	0.17	0.17	96.20	$< 10^{-6}$
	ID:Holiday	3	0.021	0.007	3.94	10^{-2}
	Residuals	197	0.35	0.002		

DoF: degrees of freedom; *SS*: Sum of Squares; *MSS*: Mean Sum of Squares; *F-stat*: experimental value of the F statistic.

places where people could stay longer than 4 h and requires that the rms value over 24 h is checked against that limit [11]. Consequently, the monitoring must be run for 24 h at each location to be checked for compliance, which is a time-consuming task. To speed up this evaluation, shorter measurements, typically performed over 6- or 30-min [1] intervals, can be done. Therefore, it is meaningful to compare short-term 6- or 30-min samples to the daily (24 h) average exposure. More formally, we introduce ΔE_{avg}, defined as

$$\Delta E_{\text{avg}} = \frac{E_{\text{avg}} - E_{24\,\text{h}}}{E_{24\,\text{h}}} \tag{1}$$

where "avg" can be equal to 6 or 30 min.

Fig. 6(a) shows boxplots of $\Delta E_{6\,\text{min}}$ by the hour of the day and by location, grouped by working days and holidays. Some interesting patterns can be observed.

1) Despite a significant data dispersion and many outliers for each time series, there is a clear day/night trend in the distribution of $\Delta E_{6\,\text{min}}$. This trend confirms that during peak hours (10 A.M. to 3 P.M.) of working days, the 6-min average tends to overestimate the 24-h average. The overestimation indeed persists from about 9 A.M. to 5 P.M. which is the period during which the first quartile of the distribution remains over zero. During holidays, overestimation tends to shift in time to later hours, being present from noon to about 10 P.M., which is consistent with the increased mobile traffic at night hours.
2) The four time series show a different distribution of $\Delta E_{6\,\text{min}}$ values during evening and night hours. In contrast, boxplots are more comparable during the day (and, in particular, during peak hours). Since the chosen time series have been measured in different urban scenarios of very different cities, this behavior seems to denote that the exposure levels during day hours tend to overestimate 24-h average exposure quite independently of the propagation scenario, the type of mobile service, and the parameters connected to traffic load of the BSs in the measurement area.

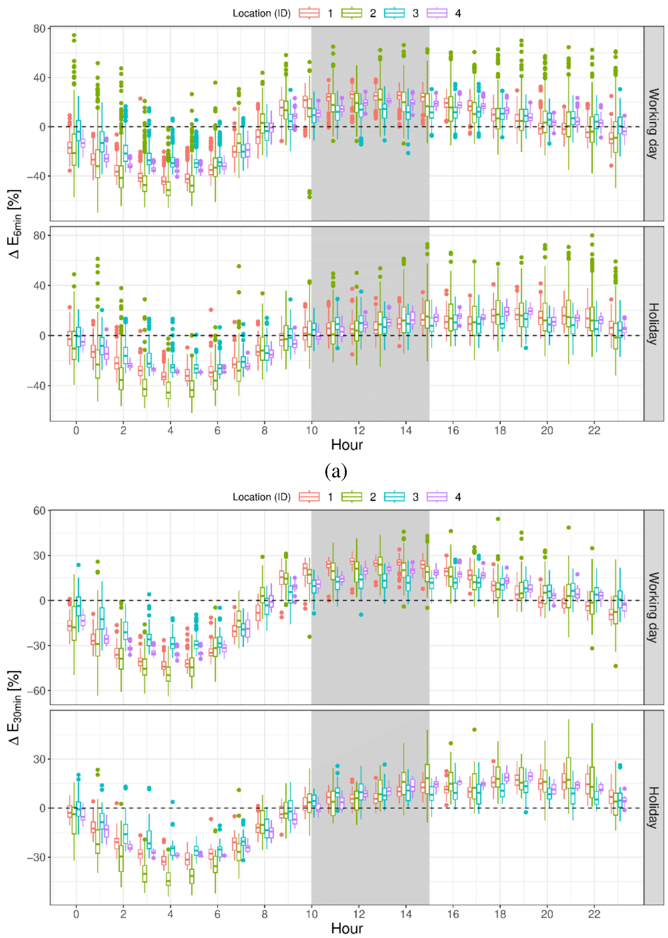

(a)

(b)

Fig. 6. Distribution of $\Delta E_{6\,\text{min}}$ and $\Delta E_{30\,\text{min}}$ by the hour of day. (a) 6-min averaging time. (b) 30-min averaging time.

Boxplots of $\Delta E_{30\,\text{min}}$ shown in Fig. 6(b) show similar behavior, although the overall spanned interval of values is tighter.

V. Extrapolation Factor

Given the similar behavior over different locations, ΔE can be profitably used to determine an appropriate *extrapolation factor* F which may serve to extrapolate 24-h measurements from 6-min samples. Such *extrapolation factor* F is, therefore, unique and it does not depend on the specific location.

Fig. 7 shows the sample distribution of $\Delta E_{6\,\text{min}}$ and $\Delta E_{30\,\text{min}}$ at 11 A.M. for both working days and holidays, obtained by grouping all available values of ΔE without distinction among locations. In the same figure, the distribution mean, median, and mode [33] are shown. By extracting these values for every hour of the day under different averaging times and types of day, we obtain the curves shown in Fig. 8, which define F based on an experimental approach. For example, if we make a 6-min measurement at a specific time of the day, we can extrapolate the 24-h value from that measurement by picking the value of F_{mo} (i.e., the value of F calculated through the mode of $\Delta E_{6\,\text{min}}$) corresponding to that hour and using the inverse formula of (1)

$$E_{24\,\text{h}} = \frac{E_{6\,\text{min}}}{1 + F_{\text{mo}}}. \tag{2}$$

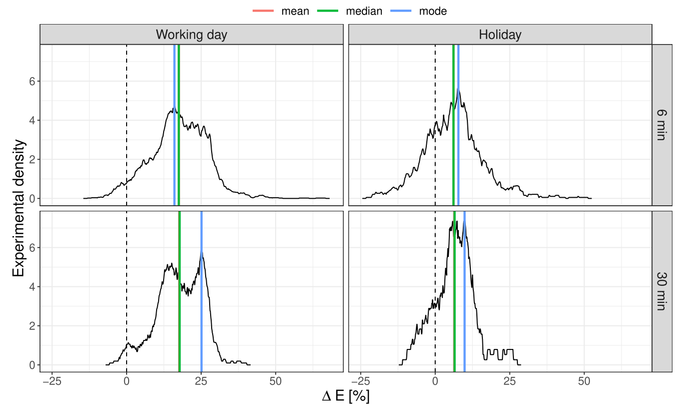

Fig. 7. Distribution of 6- and 30-min samples of ΔE at 11 A.M. for working and nonworking days.

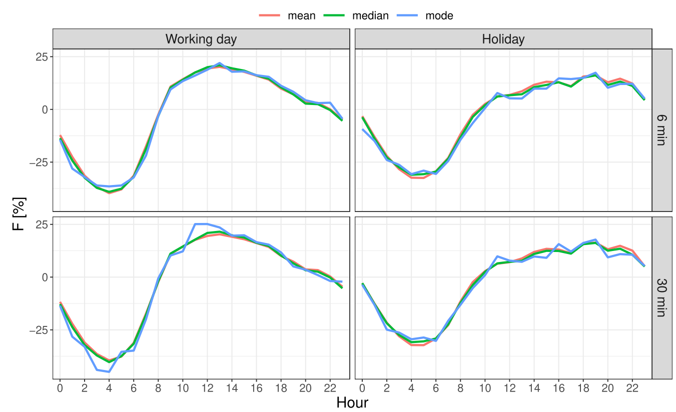

Fig. 8. Extrapolation factor for 6- and 30-min measurements on working and nonworking days.

A. Validation of F

To validate the use of the extrapolation factor, we applied F to one week of 6-min measurements extracted from the long-term time series in Fig. 2(a). The results of the extrapolation are reported in Fig. 9, where the solid red line is the actual 24-h average, while the dashed lines show the extrapolated value E_p from each 6-min measurement according to the mean, median, and mode of F.

Then, we defined the extrapolation error ϵ

$$\epsilon = E_p - E_{24\,\text{h}} \tag{3}$$

and the relative extrapolation error ϵ_r

$$\epsilon_r = \frac{E_p - E_{24\,\text{h}}}{E_{24\,\text{h}}} \tag{4}$$

where E_p is the exposure extrapolated from the 6-min measure by application of (2) and $E_{24\,\text{h}}$ is the actual 24-h average exposure. The boxplots for both quantities measured in the time interval between 10 A.M. and 3 P.M. of working days (the time interval when 6-min measurements are usually made) are presented in Fig. 10. Focusing on the range between the first and third quartiles, besides location 1 that overestimates between 0% and +10%, boxplots show that ϵ_r is on average equal to zero and spans at most the range from −10% to +10% (location 2).

By comparing ϵ_r in Fig. 10(b) with $\Delta E_{6\,\text{min}}$ for working days shown in Fig. 6(a) (which spans from +5% to +30%), we can observe that E_p is a better estimate of $E_{24\,\text{h}}$ than $E_{6\,\text{min}}$.

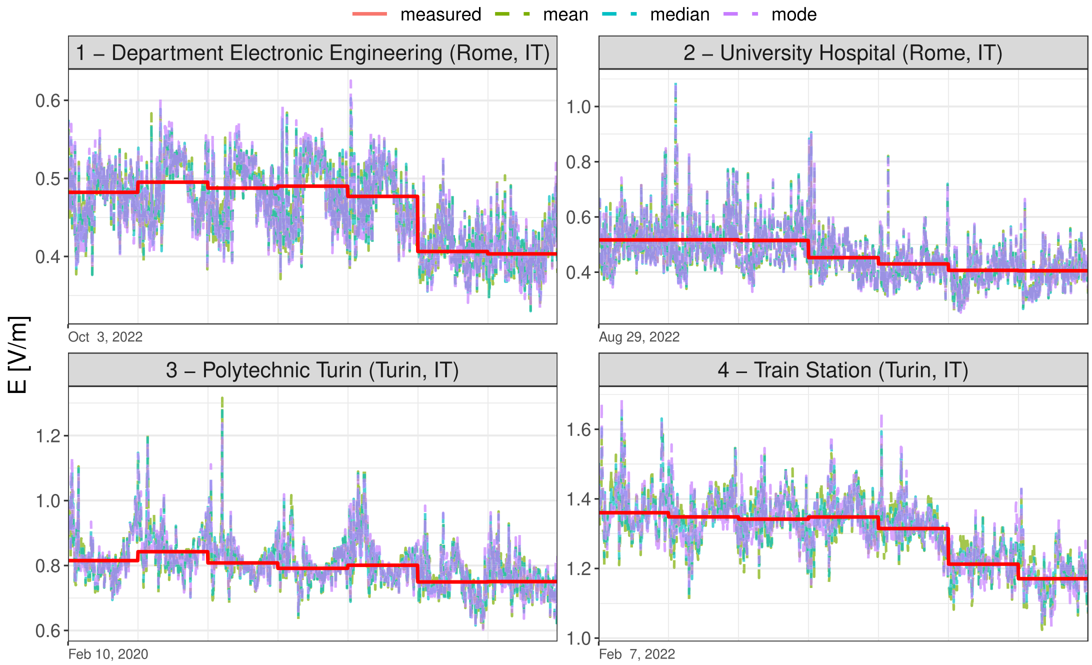

Fig. 9. Validation of extrapolation factor F.

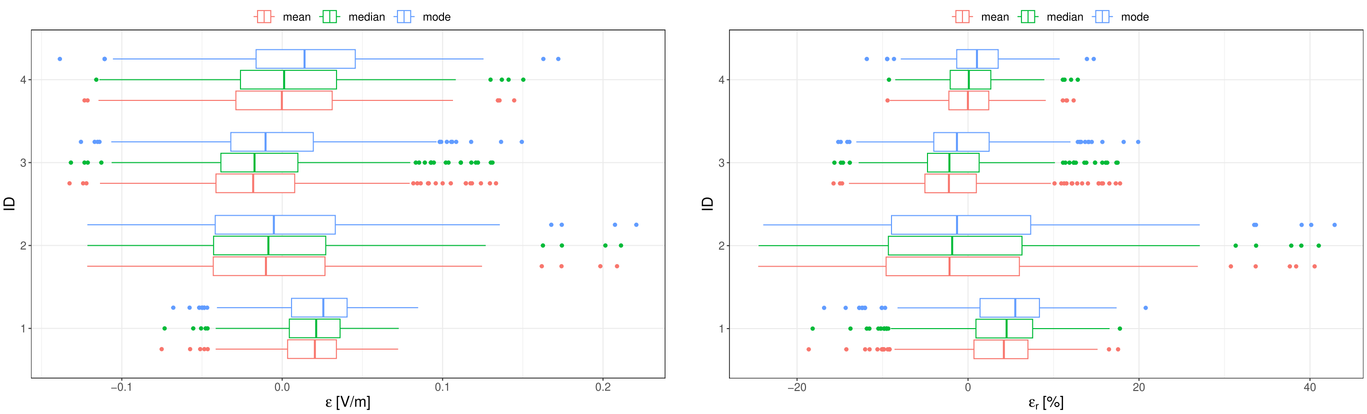

(a) (b)

Fig. 10. Extrapolation error and relative error. (a) Error. (b) Relative error.

B. Independent Validation of F

To validate the use of the extrapolation factor to estimate the $E_{24\,\mathrm{h}}$ average in a context similar to the operational ones, we applied the factor F [mean value, due to its better performance in the validation as shown in Fig. 10(b)] to three recent independent series of 6-min measurements in the city of Turin, Italy. The location and context features of the three series are similar to those used in the statistical analysis. The first series (A) covers seven days in September 2022, on an open terrace on the top of a seven-floor building in the city center, characterized by $E_{24\,\mathrm{h}}$ average of 4.45 V/m over the whole period. The second monitoring (B), carried out in early 2022, refers to a similar location but in an area devoted to commercial activities and registered a $E_{24\,\mathrm{h}}$ average of 3.28 V/m. The last one (C) covers six days in March 2023; the monitoring unit was located on the roof of an eight-floor building in the city center overlooking a quite wide square and registered a $E_{24\,\mathrm{h}}$ average of 2.57 V/m. All locations are characterized by a comparable exposure time trend over daily hours, although they are characterized by the $E_{24\,\mathrm{h}}$ average higher than that of the time series used for the estimation of the extrapolation factor estimation. We calculated the extrapolation error ϵ and the relative extrapolation error ϵ_r defined by (3) and (4). The distribution ϵ_r, considering the time interval between 10 A.M. and 3 P.M. of working days, is reported in Fig. 11. In this context, ϵ_r shows average values (8.5%, 1.7%, and 2.5%, respectively) that are larger than the reference values in Fig. 10, with extreme values spanning from -17% to 24%. Focusing on the range between the first and third quartiles, values span at most the range from -4.75% to 8% (location B). These results show a general overestimation of the $E_{24\,\mathrm{h}}$ average, with the positive mean value distribution. Even if the lower quartile is negative for locations B and C, ϵ_r is mostly toward positive values.

The behavior of the relative extrapolation error seems to be related to the $E_{24\,\mathrm{h}}$ average over the whole period: where the value is higher (location A), the relative error is also higher with all positive distribution values.

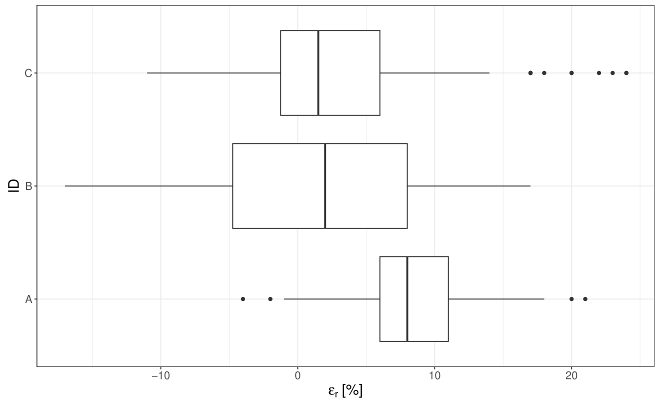

Fig. 11. Relative error distribution for locations A, B, and C.

The independent validation carries out a reliable range of variability of the $E_{24\,\mathrm{h}}$ estimation, confirming that it can be applied to get the $E_{24\,\mathrm{h}}$ preliminary estimation from single 6-min measurements.

VI. Discussion

Operators typically perform EMF measurements to measure the baseline exposure during the planning of new sites. These measurements are typically run over critical points in the neighborhood of the location that is selected to install the new antennas, which commonly already hosts radiating antennas from other operators and different technologies. In many authorization procedures, the baseline exposure level measured over the critical points is then added (in quadrature) to the estimated exposure level derived from simulations of the antennas to be installed. The total resulting exposure level is the value that is compared against the maximum exposure limit defined by law. Our work provides a new tool in this direction, although we point out that the EMF levels observed in this work are always largely lower than the maximum EMF imposed by law. Intuitively, an operator may perform a measurement over a short time scale and then refine such measurement by adopting our methodology to rescale the measured EMF over the time interval used for comparison against the limit. This step allows a better estimation of the baseline exposure and hence a more correct evaluation of the total exposure resulting from the measured and the simulated components.

VII. Conclusion and Future Work

In this article, we have focused on the problem of evaluating the average exposure over long intervals (e.g., 24 h) by measuring the EMF over shorter time scales (e.g., 6 and 30 min). To this aim, we have followed an experimental-based approach, starting from the analysis of EMF measurement campaigns in the frequency range from 100 kHz to 7 GHz. Exposure levels were sampled at various locations in two different cities in Italy over medium-to-long-term intervals spanning from a few weeks to two months. The four locations show similar statistics for 6-min and 24-h averages, with slightly larger variance in one case. Mean values differ significantly with the location and the type of the day (i.e., working day or holiday), with a strong interaction between the two terms. The comparison between 6-min and 24-h averages shows that the shorter time average typically overestimates the daily average in a wider interval than the usual peak-hours interval. This behavior is typical to all four locations sampled and is used to propose a correction factor to extrapolate daily averages from shorter-term measurements. The validation of the extrapolation factor performed on different time series confirms its suitability for the $E_{24\,\mathrm{h}}$ preliminary estimation.

In future work, we plan to extend our analysis to multiple domains. First, a further validation process, based on a higher number of independent measures, will be performed, to assess the validity of the estimation method in the operational measurement routine. Second, being a large number of shorter time series available, a statistical analysis will be carried on, to understand the influence of location metrics (e.g., geographical, urbanization level, distance from the BSs, etc.) on the extrapolation factor. Third, long-term monitoring in rural areas will be carried out, to analyze the different behavior and define a specific extrapolation factor. Fourth, a further in-depth analysis considering only the 5G monitored bands will be taken into account. This step can, for example, include the parameters that are connected to the BS traffic load in the measurement area.

References

[1] International Commission on Non-Ionizing Radiation Protection, “Guidelines for limiting exposure to electromagnetic fields (100 kHz to 300 GHz),” *Health Phys.*, vol. 118, no. 5, pp. 483–524, May 2020.

[2] A. Ahlbom et al., “Guidelines for limiting exposure to time-varying electric, magnetic, and electromagnetic fields (up to 300 GHz),” *Health Phys.*, vol. 74, no. 4, pp. 494–521, 1998.

[3] C. Apostolidis, A. Manassas, S. Iakovidis, and T. Samaras, “Electromagnetic fields in the environment: An update of monitoring networks in Europe,” in *Proc. 3rd URSI Atlantic Asia Pacific Radio Sci. Meeting (AT-AP-RASC)*, May 2022, pp. 1–3.

[4] P. Gajšek, P. Ravazzani, J. Wiart, J. Grellier, T. Samaras, and G. Thuroczy, “Electromagnetic field exposure assessment in Europe radiofrequency fields (10 MHz–6 GHz),” *J. Exposure Sci. Environ. Epidemiol.*, vol. 25, pp. 37–44, Aug. 2013.

[5] A. Manassas, A. Boursianis, T. Samaras, and J. Sahalos, “Hermes program: The Greek experience of an electromagnetic radiation monitoring system,” in *Proc. Manage. Committee Meeting Workshop Antenna Syst. Sensors Inf. Soc. Technol. COST IC*, Apr. 2008, pp. 1–21.

[6] C. Oliveira et al., “The moniT project: Electromagnetic radiation exposure assessment in mobile communications,” *IEEE Antennas Propag. Mag.*, vol. 49, no. 1, pp. 44–53, Feb. 2007.

[7] N. Djuric, D. Kljajic, T. Gavrilov, V. Otasevic, and S. Djuric, “The EMF exposure monitoring in cellular networks by serbian EMF RATEL system,” in *Proc. IEEE Int. Symp. Meas. Netw. (MN)*, Padua, Italy, Jul. 2022, pp. 1–6.

[8] D. Kljajic and N. Djuric, “Comparative analysis of EMF monitoring campaigns in the campus area of the University of Novi Sad,” *Environ. Sci. Pollut. Res.*, vol. 27, no. 13, pp. 14735–14750, May 2020.

[9] European Council, “Council recommendation of 12 July 1999 on the limitation of exposure of the general public to electromagnetic fields (0 Hz to 300 GHz) (1999/519/EC),” *Off. J. Eur. Communities*, vol. 199, pp. 59–70, Jul. 1999.

[10] *Fissazione Dei Limiti di Esposizione, Dei Valori di Attenzione e Degli Obiettivi di Qualità Per la Protezione Della Popolazione Dalle Esposizioni a Campi Elettrici, Magnetici ed Elettromagnetici Generati a Frequenze Comprese Tra 100 kHz e 300 GHz*, Off. Gazette Italian Republic, DPCM, Jul. 2003.

[11] *L 221/2012, Conversione in Legge, Con Modificazioni, Del Decreto-Legge 18 Ottobre 2012, n. 179, Recante Ulteriori Misure Urgenti Per la Crescita Del Paese*, Off. Gazette Italian Republic, Dec. 2012.

[12] D. Colombi, B. Thors, T. Persson, N. Wirén, L.-E. Larsson, and C. Törnevik, “Output power distributions of mobile radio base stations based on network measurements,” *IOP Conf. Ser., Mater. Sci. Eng.*, vol. 44, Apr. 2013, Art. no. 012016.

[13] V. Bottura, M. C. Borlino, M. Mathiou, S. Adda, S. D'Elia, and D. Vaccarono, "Measurements of electromagnetic field strength in urban environment from UMTS radio base stations and analysis of the relation with the radiated power," in *Proc. Int. Symp. Electromagn. Compat. (EMC EUROPE)*, Sep. 2012, pp. 1–4.

[14] N. Pasquino and R. Schiano Lo Moriello, "A critical note to the standard procedure for assessing exposure to GSM electromagnetic field," *Measurement*, vol. 73, pp. 563–575, Sep. 2015.

[15] N. Pasquino, "Measurement and analysis of human exposure to electromagnetic fields in the GSM band," *Measurement*, vol. 109, pp. 373–383, Oct. 2017. [Online]. Available: https://linkinghub.elsevier.com/retrieve/pii/S0263224117303858

[16] D. Colombi, P. Joshi, B. Xu, F. Ghasemifard, V. Narasaraju, and C. Törnevik, "Analysis of the actual power and EMF exposure from base stations in a commercial 5G network," *Appl. Sci.*, vol. 10, no. 15, p. 5280, Jul. 2020.

[17] A. Schiavoni, S. Bastonero, R. Lanzo, and R. Scotti, "Methodology for electromagnetic field exposure assessment of 5G massive MIMO antennas accounting for spatial variability of radiated power," *IEEE Access*, vol. 10, pp. 70572–70580, 2022.

[18] G. Betta, D. Capriglione, G. Cerro, G. Miele, M. D. Migliore, and D. Šuka, "Experimental analysis of 5G pilot signals' variability in urban scenarios," in *Proc. IEEE Int. Symp. Meas. Netw. (MN)*, Jul. 2022, pp. 1–6.

[19] L. Chiaraviglio, A. Elzanaty, and M.-S. Alouini, "Health risks associated with 5G exposure: A view from the communications engineering perspective," *IEEE Open J. Commun. Soc.*, vol. 2, pp. 2131–2179, 2021.

[20] P. Bienkowski and B. Zubrzak, "Electromagnetic fields from mobile phone base station—Variability analysis," *Electromagn. Biol. Med.*, vol. 34, no. 3, pp. 257–261, Jul. 2015.

[21] D. Šuka, P. Pejović, and M. Simić-Pejović, "Application of time-averaged and integral-based measure for measurement results variability reduction in GSM/DCS/UMTS systems," *Radiat. Protection Dosimetry*, vol. 187, no. 2, pp. 191–214, Dec. 2019.

[22] A. B. Olorunsola, O. M. Ikumapayi, B. I. Oladapo, A. O. Alimi, and A. O. M. Adeoye, "Temporal variation of exposure from radio-frequency electromagnetic fields around mobile communication base stations," *Sci. Afr.*, vol. 12, Jul. 2021, Art. no. e00724.

[23] P. Frei et al., "Temporal and spatial variability of personal exposure to radio frequency electromagnetic fields," *Environ. Res.*, vol. 109, no. 6, pp. 779–785, Aug. 2009.

[24] L. E. Birks et al., "Spatial and temporal variability of personal environmental exposure to radio frequency electromagnetic fields in children in Europe," *Environ. Int.*, vol. 117, pp. 204–214, Aug. 2018.

[25] S. Aerts, J. Wiart, L. Martens, and W. Joseph, "Assessment of long-term spatio-temporal radiofrequency electromagnetic field exposure," *Environ. Res.*, vol. 161, pp. 136–143, Feb. 2018.

[26] M. Velghe, W. Joseph, S. Debouvere, R. Aminzadeh, L. Martens, and A. Thielens, "Characterisation of spatial and temporal variability of RF-EMF exposure levels in urban environments in Flanders, Belgium," *Environ. Res.*, vol. 175, pp. 351–366, Aug. 2019.

[27] S. Aerts et al., "Lessons learned from a distributed RF-EMF sensor network," *Sensors*, vol. 22, no. 5, p. 1715, Feb. 2022.

[28] V. Raida, P. Svoboda, M. Koglbauer, and M. Rupp, "On the stability of RSRP and variability of other KPIs in LTE downlink—An open dataset," in *Proc. IEEE Global Commun. Conf. (GLOBECOM)*, Dec. 2020, pp. 1–6.

[29] L. Chiaraviglio et al., "Massive measurements of 5G exposure in a town: Methodology and results," *IEEE Open J. Commun. Soc.*, vol. 2, pp. 2029–2048, 2021.

[30] L. Chiaraviglio, C. Lodovisi, D. Franci, S. Pavoncello, and T. Aureli, "Six months in the life of a cellular tower: Is 5G exposure higher than pre-5G one?" in *Proc. IEEE Int. Symp. Meas. Netw. (MN)*, Jul. 2022, pp. 1–6.

[31] P. De Lellis, F. L. Iudice, and N. Pasquino, "Time-Series-Based model and validation for prediction of exposure to wideband radio frequency electromagnetic radiation," *IEEE Trans. Instrum. Meas.*, vol. 69, no. 6, pp. 3198–3205, Jun. 2020.

[32] J. A. Gubner, *Probability and Random Processes for Electrical and Computer Engineers*. Cambridge, U.K.: Cambridge Univ. Press, 2006.

[33] D. Montgomery, *Statistical Quality Control: A Modern Introduction*, 7th ed. Hoboken, NJ, USA: Wiley, 2012.

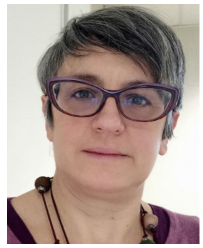

Sara Adda received the M.Sc. degree (cum laude) in physics and the master's degree in health physics from the University of Turin, Turin, Italy, in 1998 and 2003, respectively.

From 1998 to 1999, she has worked with the ENEA Casaccia Research Center, Rome, Italy, for one year, in the Interdepartmental Computing and High-Performance Networks Project, implementing a system for the simulation of electromagnetic field (EMF) dynamics in complex environments through the use of massively parallel architectures. Since 1999, she has been working with the Physical and Technological Risk Department, Regional Agency for Environmental Protection of Piedmont (ARPA Piemonte), Ivrea, Italy, dealing with the control and monitoring of non-ionizing radiation and the development of theoretical forecasting/numerical calculation methods, both in the low- and high-frequency ranges. She currently participates in the Italian Electrotechnical Committee (CEI) working groups, for the drafting of technical standards on measurement and evaluation methods for human EMF exposure. She also deals with the theoretical and practical aspects related to the measurement of EMFs in the workplace. In this context, she is the Representative of the Piedmont Region in the Interregional Technical Coordination Group. She also participates in European (Twinning Italy-Poland Project) and international collaborative projects (ARPA Piemonte—Beijing Municipal Environmental Protection Bureau), on methods and techniques for measuring and evaluating human exposure to EMF both in the workplace and in the living environment.

Luca Chiaraviglio (Senior Member, IEEE) received the Ph.D. degree in telecommunication and electronics engineering from the Polytechnic University of Turin, Turin, Italy, in 2011.

He is currently an Associate Professor with the University of Rome "Tor Vergata," Rome, Italy, teaching the courses of "Internet of Things" and "Networking and Internet." He has coauthored more than 160 articles published in international journals, books, and conferences. His current research interests include 6G networks, electromagnetic field assessments of 5G networks, and health risks assessment of 5G communications.

Dr. Chiaraviglio has received the Best Paper Award at the IEEE Vehicular Technology Conference (VTC Spring) in 2020 and 2016 and the Conference on Innovation in Clouds, Internet and Networks (ICIN) in 2018, all of them appearing as the first author. Some of his papers are listed as the Best Readings on Green Communications by the IEEE. Moreover, he has been recognized as an author in the top 1% most highly cited papers in the information and communication technology (ICT) field worldwide and the top 2% world scientists according to the 2021 and 2022 updates of the science-wide author databases of standardized citation indicators. He serves as the Chief Editor for the *Frontiers in Communications and Networks* journal—Networks Section, the Dean's Delegate at the CNIT Shareholders Assembly, a TPC Member for the IEEE INFOCOM conference (since 2019), a Coordinator of activities for the RESTART Project at the Research Unit, University of Rome "Tor Vergata," and a Co-Principal Investigator for the CNIT-KAUST Bilateral Project PLAN-EMF.

Daniele Franci received the M.Sc. (magna cum laude) and Ph.D. degrees in nuclear and subnuclear physics from the Sapienza University of Rome, Rome, Italy, in 2007 and 2011, respectively.

From 2009 to 2011, he was an Analyst Technologist with Nucleco SPA, Rome, involved in radiological characterization of radioactive wastes from the decommissioning of former Italian nuclear power plants. He joined ARPA Lazio, Rome, in 2011, being involved in radio-frequency (RF) electromagnetic field (EMF) human exposure assessment. Since 2017, he has been involved in activities of the Italian Electrotechnical Committee (CEI) for the definition of technical procedures for EMF measurement from 4G/5G MIMO sources.

Chiara Lodovisi received the Ph.D. degree in engineering electronics from the University of Rome "Tor Vergata," Rome, Italy, in 2020.

She has worked for five years as a Radio Frequency (RF) Engineer Consultant for H3G mobile operator and then as a Research Associate with the University of Rome "Tor Vergata," focusing on optical communications, submarine and satellite optical links, and radio over fiber. She is currently a Researcher with the National Inter-University Consortium for Telecommunications (CNIT), Parma, Italy. Her research interests include 5G networks, health risk assessment of 5G communications, interoperability over fiber between TETRA/LTE systems, and 5G networks.

Nicola Pasquino (Senior Member, IEEE) was born in Naples, Italy, in 1973. He received the M.Sc. degree (magna cum laude) in electronics engineering and the Ph.D. degree in information engineering from the Università degli Studi di Napoli Federico II, Naples, in 1998 and 2002, respectively.

He was a Fulbright Scholar with the University of Pennsylvania, Philadelphia, PA, USA, from 2000 to 2001. He is currently a Professor of electrical and electronic measurements with the Department of Electrical Engineering and Information Technologies, Università degli Studi di Napoli Federico II, where he is also the Chief Scientist of the Electromagnetic Compatibility Laboratory. His research interests include electromagnetic compatibility measurements and measurements of human exposure to high-frequency electromagnetic fields, with the application of machine-learning methodologies to measurement data analysis.

Prof. Pasquino was the President of the Rotary Club Napoli Angioino (D2101, Italy) from 2019 to 2020. He has been a member of Rotary since 2005. He is the Chair of the TC106 "Human Exposure to Electromagnetic Fields" of the Italian Electrotechnical Committee (CEI). He is also the Chair of the Committee on "Human Exposure to Electromagnetic Fields" within the Engineering Register of Naples. He is also a member of the Editorial Board of the *Measurement Science Review* journal. He serves as an Editor for the *Journal of Electrical and Computer Engineering* and a Section Editor for the *Acta IMEKO* journal.

Settimio Pavoncello was born in Rome, Italy, in 1973. He received the M.Sc. degree in telecommunication engineering from the Sapienza University of Rome, Rome, in 2001.

Since 2002, he has been working with the Electromagnetic Field (EMF) Department, Regional Environmental Agency of Lazio, Rome. He specializes in EMF measurements and EMF project evaluation related to radio, TV, and mobile communications systems maturing huge experience in the use of broadband and selective instruments. In the last years, he has deepened the issues related to measurements on LTE and the NB-IoT signals.

Mr. Pavoncello, since 2018, has been actively involved in the Working Group "Mobile Base Stations" within the Technical Committee 106 of the Italian Electrotechnical Committee (CEI) aimed at defining measurement procedures for mobile communications signals and is currently engaged in various projects concerning measurement on 5G signals.

Chiara Pedroli received the M.Sc. degree (cum laude) in environmental and biomedical physics from the University of Turin, Turin, Italy, in 2010.

She has worked for some years in startups dealing with temporary management and local development projects. Since 2018, she has been working with the Physical and Technological Risk Department, Regional Agency for Environmental Protection of Piedmont (ARPA Piemonte), Ivrea, Italy. She is involved in electromagnetic field measurements and human exposure assessment, related to mobile communications systems and low-frequency sources. She is also in charge of data public dissemination related to electromagnetic field monitoring and control, through a dedicated geographic information system.

Renata Pelosini received the M.Sc. degree in physics from the University of Milan, Milan, Italy, in 1990.

She has worked many years in the weather forecasting field, developing excellent expertise in meteorological modeling and data statistical analysis. Since 2021, she has been working with the Physical and Technological Risk Department, Regional Agency for Environmental Protection of Piedmont (ARPA Piemonte), Ivrea, Italy, dealing with the control and monitoring of nonionizing radiation and the measure of individual exposure to radio-frequency (RF) electromagnetic fields, dealing with projects aimed to evaluate their health impacts.

Open Access funding provided by 'Università degli Studi di Napoli "Federico II"' within the CRUI CARE Agreement